Nigerian Journal of Physics (NJP)
ISSN online: 3027-0936
ISSN print: 1595-0611
DOI: 4https://doi.org/10.62292/njp.v33i3.2024.302
Volume 33(3), September 2024

Design of High Performance Graphene Thin Films Perovskite Solar Cells by Numerical Modeling Based on Coupled Differential Equations

***[1]Ladan, H. M. A., [2]Buba, A. D. A., [3]Umar, M. and [4]Adamu, A. S.**

[1]Department of Physics, Faculty of Science, Sa'adu Zungur University, Bauchi State, Nigeria
[2]Department of Physics, Faculty of Science, University of Abuja, Abuja.
[3]Department of Electrical Engineering, Ahmadu Bello University, Zaria, Nigeria
[4]Department of Chemistry, Faculty of Science, University of Abuja, Abuja, Nigeria

[*]Corresponding author's email: Ladan@basug.edu.ng; Ladansons@gmail.com

ABSTRACT

In this study, graphene a two dimensional nanomaterial was prepared by modified Hummer's method and the optical properties were explored using UV-visible spectroscopy to determine absorption coefficients at different wavelengths based on Beer-Lambert's law. Graphene based lead-free methyl ammonium germanium halide solar cell was designed in the second stage using graphene oxide (GO) as carrier absorbers and transporters. Numerical modelling of the device in solar capacitance stimulating (SCAPS 1D) program based on second order differential equation was done. A photovoltaic parameters of 0.6227 V, 38.58 $mAcm^{-2}$, 83.07 %, 19.95 % were recorded as the open-circuit voltage, current density, fill factor and power conversion efficiency (PCE) for FTO/GO/Perovskite/Cu_2O/Au. Using the same settings for the second design, the Au/spiro-ometad/$FASnI_3$/TiO_2/FTO, the current density increases sharply from 0.50 V and with valence and conduction band at -0.35 eV and 1.78 eV respectively. The light transmittance and heat distribution across the device determine by origin pro-version 9.8.0200 indicated uniform transmission and absorption. The study showed that the presence of graphene, improved the optical transparency and enhanced carrier generation and interaction between other layers which optimized the electrical conductivity and efficiency of the solar cells when compared to previous studies in the literature. The results emphasized a viable approach in the design of efficient and stable solar cells at a reduced cost and optical losses. If mass produced can be deployed commercially due to enhanced solar energy absorption potential ahead of the Si based PVCs.

Keywords:
Optical Property,
Graphene,
Perovskite,
Solar Cells,
SCAPS,
Numerical modeling.

INTRODUCTION

Due to increasing energy demand worldwide, studies on improving the performance of photovoltaic (PV) devices are on the increase (Mahajan et al, 2020). Integration of carbon based material in designing solar cells improved efficiency, reduced cost and enhanced life time (Iqbal et al., 2019). Graphene is a single layer of graphite and is sp^2 hybridized carbon atoms in hexagonal form. It has high electronic conductivity at room temperature. The thermal conductivity is 3.0×10^3 Wm/K and the transmittance is about 90% (Geim et al., 2007; Kumar et al., 2019). Graphene oxide (GO) has carboxyl, epoxy and hydroxyl functional groups (Paulchamy et al., 2015). It has very large surface area (2630 m^2/g).

Perovskite material can be represented by the formula ABX_3 where A is a cation (A^+), an organic methyl ammonium (MA), formamidinium (FA) or Cesium (Cs) ions. B is a heavy metal such as Pb, Ge or Sn, while X^- is a halide anion (I, Br, Cl, or their mixtures). Perovskite solar cells (PSCs) suffers from drawbacks due to low electron mobility in the metallic semiconducting components (SMO_X) such as TiO_2, SnO_2 and ZnO with a higher density of electronic trap states, instability under UV visible light, poisonous lead, hysteresis, and operational life-time. The excessive energy loss due to the transmission and thermalization of hot carriers can be minimized by sandwiching carbon or polymers in between the layers (Hu et al., 2019; Tress et al., 2019; Wali et al., 2018). The development of lead-free PSCs

are in progress due to increase in energy demand and the need to cut the use of fossil fuels. Carbon based GO improves the performance of PV devices by enhancing the photo-generated electrons since the carbon molecules absorb light energy in the UV-visible range at different wavelengths (Chou et al., 2016). Adding absorption coefficient (α) profile into photovoltaic (PV) devices at UV-visible range from 200 nm to 800 nm is vital for the optimum performance of optoelectronic and PV cells (Chou et at., 2016; Alam et al., 2017; Chou et al., 2020).

Pulson's group in 2003 performed an optical characterization of $Cu(In,Ga)Se_2$ (CIGS) alloy thin films by spectroscopic ellipsometry technique (Pulson et al., 2003). In 2017, Kim et al. extrapolated the absorption coefficients of the $Cu(In,Ga)Se_2$ from Pulson's study for the simulation of chalcopyrite dual-junction based tandem solar cells. The result showed a strong correlation between its bandgap and efficiency (Kim, 2017; Hu et al., 2019). Several studies on PSCs (Agresti et al., 2016; Elseman et al., 2017; Gagandeep et al., 2020; Dadashbeik et al., 2020; Daraie et al., 2020) have been performed without adding the absorption coefficient (α) profile to the device. It is known that optical properties of nanomaterials are enhanced by the nature of the band gap, absorption coefficient, and carrier diffusion length (100-1000 nm) (Hummer et al., 1958; Marcano et al., 2010). This can improve the carrier transport, and the photovoltaic parameters (Kumar et al., 2018; Yang et al., 2019). There were no records on the measurement and incorporation of the absorption data into photovoltaic device especially GO in PSCs as an absorber or carrier transport layer (Hummers et al., 1958; Marcano et al., 2010; Hazeghi et al., 2019; Haidari et al., 2019).

In this study, GO was prepared by modified Hummer's method and the optical properties were explored using UV-visible spectroscopy to determine absorption coefficients at different wavelengths based on Beer-Lambert's law. The data were incorporated in the design of lead-free methyl ammonium germanium halide solar cell using GO as carrier transporters in SCAPS 1D simulation software.

MATERIALS AND METHODS

Materials

Synthetic graphite (Sigma Aldrich), H_2SO_4, $NaNO_3$, HNO_3, HCl, $KMnO_4$, and distilled water. All the chemicals used were of analytical grade and were used without further purification. The fluorine doped tin oxide (FTO) glass substrates (Solaronix, Switzerland).

Modified Hummer's Method

GO was synthesized by mixing 5 g of graphite powder and conc. H_2SO_4 and HNO_3 in the ratio (3:1) in a 500 ml beaker and was sonicated for 30 min. 6 g of $KMnO_4$ was added gradually and stirring continued in an ice bath for 30 minutes. Then the mixture was kept on a magnetic stirrer at 200 rpm and the temperature was increased to 30 ^{0}C. A brown colouration was formed. The temperature was raised to 80 ^{0}C and a bright-yellow suspension was formed. When 30 ml H_2O_2 (30%) was added, it changes to golden yellow solution. After centrifugation, dilute HCl was used to wash the resultant product and properly rinsed with deionized water. 0.5 g of the synthesized GO was annealed at 150 ^{0}C for 20 minutes (figure 1 a and b). 0.2 g was coated on gold substrate for characterization and subsequent production of GO thin films on FTO glass substrate (solaronix), the procedure was adopted from Ladan and Buba, 2021.

Optical Characterization and Simulation

The absorbance values of the GO were determined using UV visible spectrophotometer (T80+) at Nile University labouratory, Abuja to provide the data in the design of lead-free methyl ammonium germanium halides using GO as carrier transporter and optimizers for a hassle free hole and electron transfers.

Solar Capacitance Stimulation

Numerical modeling were performed using SCAPS version 3.3.09 under AM 1.5 solar spectrum at 100 mW/cm^2 light intensity to obtain the photovoltaic characteristics. SCAPS can simulate the electric field distribution, current density, transport properties, carrier generation and recombination profile for thin films solar cells (Burgelman et al., 2000). The Poisson equation relates the static electric field ε to the space-charge density ρ. The electron and hole transport equations (2 and 3) are coupled by ε to form a set of coupled differential equations.

$$\frac{d^2\emptyset(x)}{dx} = -\frac{d\,\varepsilon(x)}{dx} = -\frac{\rho(x)}{\epsilon_0\epsilon_s} \quad (1)$$

Where $\emptyset$ is the electrostatic potential, ϵ_0 is the permittivity of free space and ϵ_s is the static relative permittivity of the medium.

$$D_e\frac{d^2n}{dx^2} + \mu_e\varepsilon\frac{dn}{dx} + n\mu_e\frac{d\varepsilon}{dx} - R_e(x) + G_e(x) = 0 \quad (2)$$

$$D_h\frac{d^2p}{dx^2} + \mu_h\varepsilon\frac{dn}{dx} + p\mu_h\frac{d\varepsilon}{dx} - R_h(x) + G_h(x) = 0 \quad (3)$$

Where e and p are the electron and hole densities, μ_e and μ_p represents the electron and hole mobilities, D_e and D_h are the electron and hole diffusion constants, R(x) and G(x) denotes the recombination and photo-generation rates, respectively.

As shown in figure 1c, the device is a thin film solar cell which was modelled as a stack of layers characterized by the thickness, doping level, charge mobility, absorption coefficient and other physical properties of the material. The two configuration tested are

FTO/GO/Perovskite/Cu_2O/Au and FTO/GO/TiO_2/Perovskite/Spiro-OMETAD/Au.

The absorption coefficient was set at 105 cm^{-1} and the operating temperature at 300 K while that of GO was incorporated between 200 and 800 nm to improve the carrier absorption and transportation.

The measured absorption coefficient $\alpha(t)$ (cm^{-1}) of GO at different wavelengths) can be related to the transmittance (t) by

$$\alpha(t) = \frac{1}{d}\ln\frac{1}{t} \quad (4)$$

Where $t = 10^{-A}$, d is the thickness of the thin film and A is the absorbance of the sample.

GO thin films (Eg = 2.55 eV) were prepared on gold substrate, the absorption coefficient α (Eluyemi et al., 2016; Kim, 2017) can be expressed as:

$$\alpha(v)hv = B(hv-E_g)^n \quad (4)$$

Where B is constant ~ 1, α is the absorption coefficient, E_g is the energy band gap, n is between ½ and 3 depending on the transition, in this case n is 2.

Table 1 shows parameters that were collected from recent studies. These include band gap energy (E_g), electron affinity (χ), relative dielectric permittivity (ε_r), mobility of electron (μ_n) mobility of hole (μ_p) and defect density (Ntm), N_c(cm^{-3}) is effective density of states at CB, N_v (cm^{-3}) is the effective density of states at VB, N_d (cm^{-3}) is the donor density /density of p-type doping, N_A (cm^{-3}) is the acceptor density/ density of n-type doping, ε_r is the relative dielectric permittivity, μ_n ($cm^2c^{-1}s^{-1}$) is the mobility of electron, μ_h ($cm^2c^{-1}s^{-1}$) is the mobility of electron, N_{te} (cm/s) is the electron thermal velocity, N_{th} (cm/s) is the hole thermal velocity.

Light transmittance and heat distribution across the device

To show the light transmittance and heat distribution across the device, origin pro-version 9.8.0200 was used for the heat distribution and contour map for the absorbance versus the wavelength of the radiation and the 2D heat map for the transmittance against wavelength.

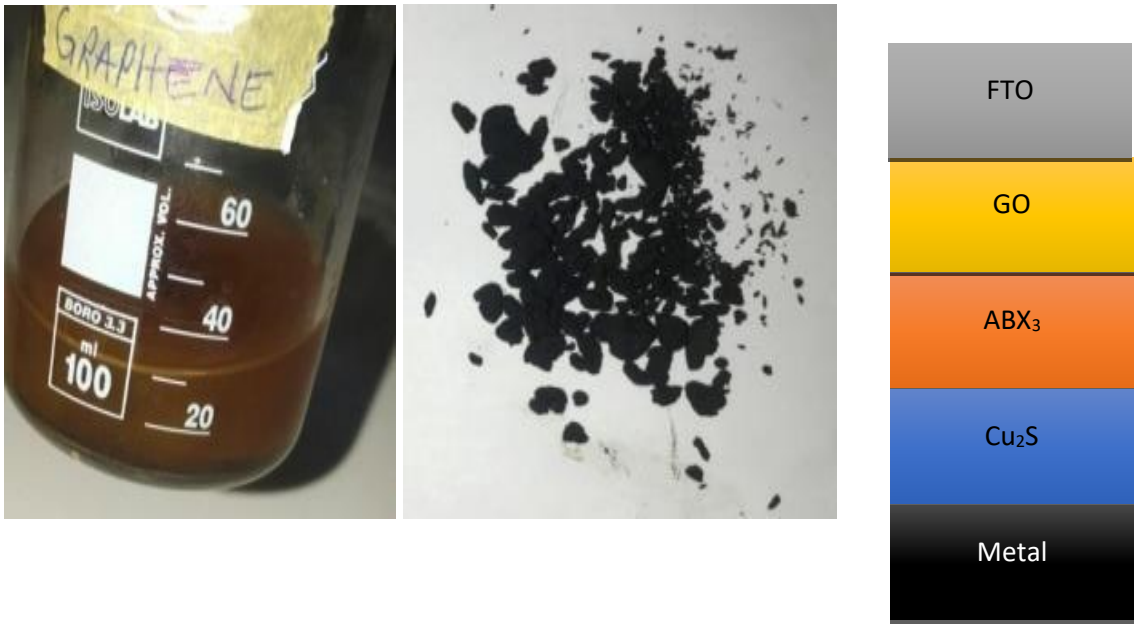

(a) (b) (c)

Figure 1: Graphene in (a) Solution (b) Lump form (c) PSCs thin films

RESULTS AND DISCUSSION

As shown in figure 1a, b and c, (a) is the GO in solution and (b) in lump form which is integrated into a heterojunction (p-i-n) solar cell (c). Electrons are collected at the fluorine doped tin oxide (FTO) and holes at the metal with high work functions as back contact such as Au. The device has intrinsic perovskite absorber layer (non-doped) between an electron transport layer n-type GO and GO-TiO_2 and hole transporting layer p-type Cu_2O and Spiro-OMeTAD with the absorption coefficient of GO incorporated the operating temperature at 300 K.

The optical absorbance coefficient of a semiconductor close to the band edge can be expressed by (1). The n depends on the nature of the transitions and the values can either be ½, 2, 3/2 or 3. It denotes allowed direct, allowed indirect, forbidden direct and forbidden indirect transitions respectively (Baharin et al., 2020).

The effect was observed from 200 nm to 800 nm at different wavelengths and absorption coefficient (α) in SCAPS software to record the photovoltaic characteristics, the current density and energy band diagram (a) Efficiency of the device (b) The energy band diagram (Figure 2a and 2b).

The data in the design of lead-free methyl ammonium germanium halides using GO as carrier transporter and optimizers for a hassle free hole and electron transfers. For the first configuration, a 0.6227 V, 38.58 $mAcm^{-2}$, 83.07 %, 19.95 % were recorded as the open-circuit voltage, current density, fill factor and power conversion efficiency for FTO/GO/Perovskite/Cu_2O/Au system and for the second configuration, FTO/GO/TiO_2/Perovskite/Spiro-OMETAD/Au a 0.6659V, 10.77$mAcm^{-2}$, 79.19%, 22.91% were obtained for the first time. The values showed enhanced photovoltaic parameters.

The presence graphene as contact /TCO layer improves the optical transparency since it can absorbs 2.3% of incident light. It transfers 97% of incident light to the active layer which consequently leads to the increase in carrier generation and enhances the interaction between the other layers. This optimizes the electrical conductivity and efficiency of solar cells (Geim et al., 2007; Gagandeep et al., 2020; Dadashbeik et al., 2020).

The Electron transporting layer (ETL) plays a vital role in the exciton separation and charge transport. TiO_2 is widely used as the ETL in PSCs. It has suitable band gap, excellent photo-electrochemical stability, and simple preparation process. The use of GO-TiO_2 as ETLs films increase the charge collection efficiency and reduce recombination occurring at the interfaces (Zhang et al., 2018; Lee et al., 2019). Photovoltaic parameters obtained were compared with similar studies available in the literature (Table 2).

The transmitted light and heat distribution showed the absorbance versus the wavelength of the radiation while the 2D heat map showed the transmittance against wavelength indicated peak heat generation at 700 nm/tr between 0.5 and 0.25 above violet at the same projection (700 nm) for the 3D surface plot. While polar contour in terms θ(x) r(Y) revealed possible angle that solar cell can be tilted to achieve maximum absorbance (table 3) and transmittance at 550.5 nm in line with (figure 3) the generation and recombination profile (Ladan and Buba, 2021).

For the second design, the Au/spiro-ometad/$FASnI_3$/TiO_2/FTO the current density increases sharply from 0.50 V (figure 5) and with valence and conduction band at -0.35 eV and 1.78 eV (figure 3.) The occupation probability of deep defect for electrons and the carrier density is showed in figure 4. The generation and recombination profile recorded peak at 1.0μm, electron capture (dark), peak electron-hole generation (green), hole and electron emission (pink and blue) (figure 4). The optical absorption of the ITO/FTO layer and the J-V characteristics curve for second configuration are indicated in Figure 5 showing the optical absorption of the ITO/FTO layer and the J-V characteristics curve. The variation of PCE (a) and the quantum efficiency (QE) with different absorber thickness between 100 and 1000 nm revealed convergence close at about 95% (Figure 6).

Table 1: Material property for each layer of the PSCs

	ITO	**Spiro-Ometad**	**$FASnI_3$**	**TiO_2**	**$MAGeI_3$**	**Graphene**
Thickness, nm	500	WR	WR		WR	WR
E_g(eV)	3.65	2.9	1.3	3.2	1.90	2.7
x (eV)	4.80	2.2	4.17	3.9	3.98	4.5
N_c(cm^{-3})	5.8 x10^{18}	2.5x10^{20}	1x10^{18}	10^{19}	10^{16}	3.10 x 10^{19}
N_v (cm^{-3})	10^{18}	2.5x10^{20}	1.0 x10^{19}	10^{19}	10^{15}	3.10 x 10^{19}
N_d (cm^{-3})	10^{20}	-	-	10^{17}	10^{9}	
N_A (cm^{-3})	0	1x10^{18}	-	-	10^{9}	0
ε_r	8.90	3	6.5	32	10	3.3
μ_n ($cm^2c^{-1}s^{-1}$)	10.0	0.0021	1.6	162x10^3	16.20	15,000
μ_h ($cm^2c^{-1}s^{-1}$)	10.0	0.0021	1.6	101x10^3	10.10	15,000
Defect density	-	-	1.6 x10^6		10^{14}	1 x 10^{15}
Work function	-	-	1.6 x10^6		-	4.0
References	Kumar et al, 2020; Rai et al, 2020	Mandadapu et al., 2017 ; Zhao et al., 2018;	Mandadapu et al., 2017; Kanoun et al., 2019	Kanoun et al., 2019	Lakhdar et al, 2019	Sutar et al, 2012; Mudd et al, 2015; Wang et al, 2020

Table 2: Photovoltaic parameters of the solar cells compared with similar studies

Structure	J_{sc} (mA/cm^2)	V_{oc} (V)	FF (%)	PCE (%)	References
FTO/GO/Perovskite/Cu_2O/Au	38.58	0.6227	83.07	19.95	This study
FTO/GO/TiO_2/Perovskite/Spiro-OMETAD/Au	10.77mAcm^{-2}	0.6659	79.19	22.91	This study
mTiO_2+G/perovskite/GO/spiro OMeTAD	22.48	1.08	75.12	18.19	Lakhdar et al., 2019
$FAPbI_3$-based Simulation	16.60	0.60	40.60	4.3	Karthick et al., 2020
$FAPbI_3$ Experimental	20.60	1.10	47.40	11.5	
$MAPbI_3$-based Simulation	23.34	1.15	70.31	18.92	Rai et al., 2020
$MAPbI_3$-based experimental	22.30	1.11	74.50	18.40	Rao et al., 2016
$CH_3NH_3PbI_3$-based experimental	18.20	0.93	71.20	12.10	Zhu et al., 2016
$CH_3NH_3PbI_3$-based solar cell Simulation, TiO_2	23.44	0.93	60.75	13.30	Agresti et al., 2016
P-graphene/$CH_3NH_3PbI_3$/n-cSi	30.87	0.6879	84.31	17.90	Gagandeep et al., 2020

Table 3: Absorption coefficient α at different thicknesses (*t*) (cm^{-1}) of GO and wavelengths

λ (nm)	GO(A)	t(GO)	d = 50nm	d = 100nm	d = 200nm
200	0.172	0.6730	7922320	3961160	1980580
300	0.667	0.2153	30722020	15361010	7680505
400	0.650	0.2239	29939000	14969500	7484750
500	1.472	0.0337	67800320	33900160	16950080
600	1.723	0.0189	79361380	39680690	19840345
700	1.761	0.0173	81111660	37331630	20277915
800	1.629	0.0235	75031740	37515870	18757935

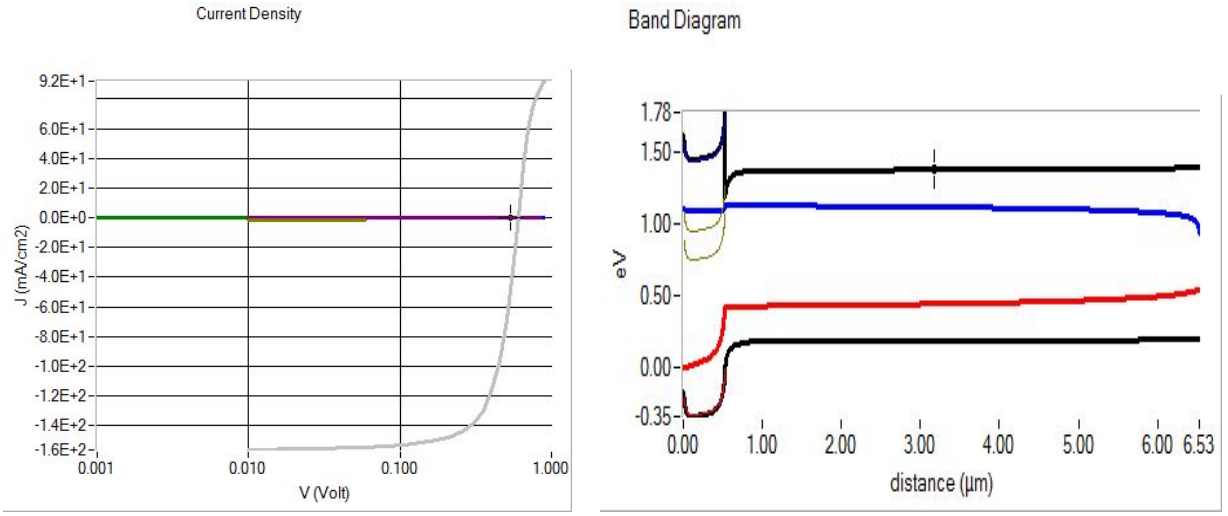

(a) (b)

Figure 2: The current density and energy band diagram

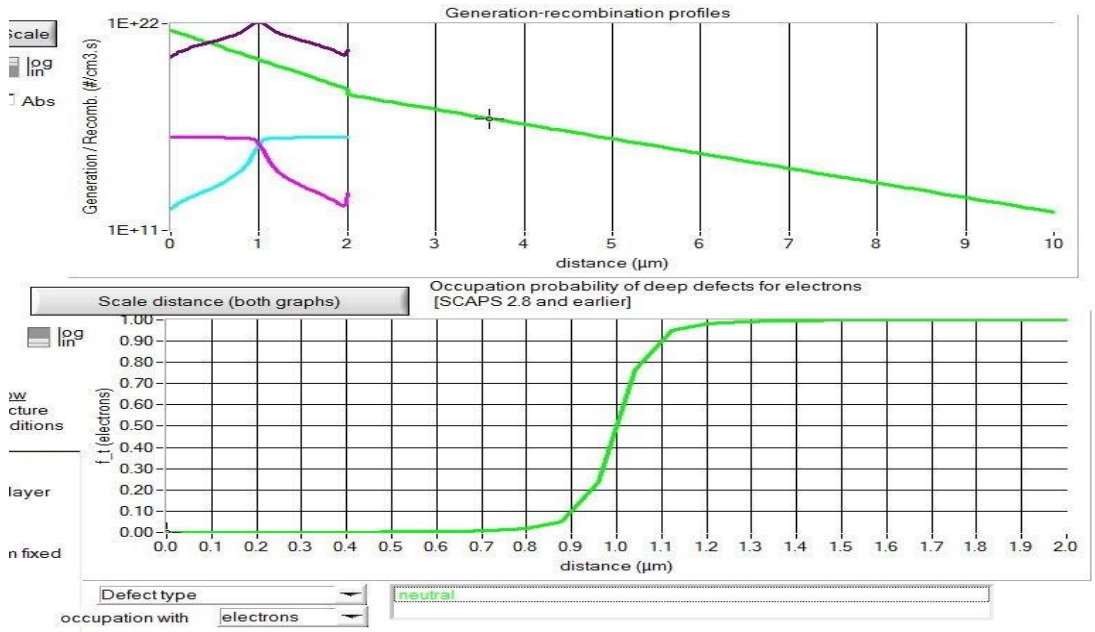

Figure 3: Generation and recombination profile

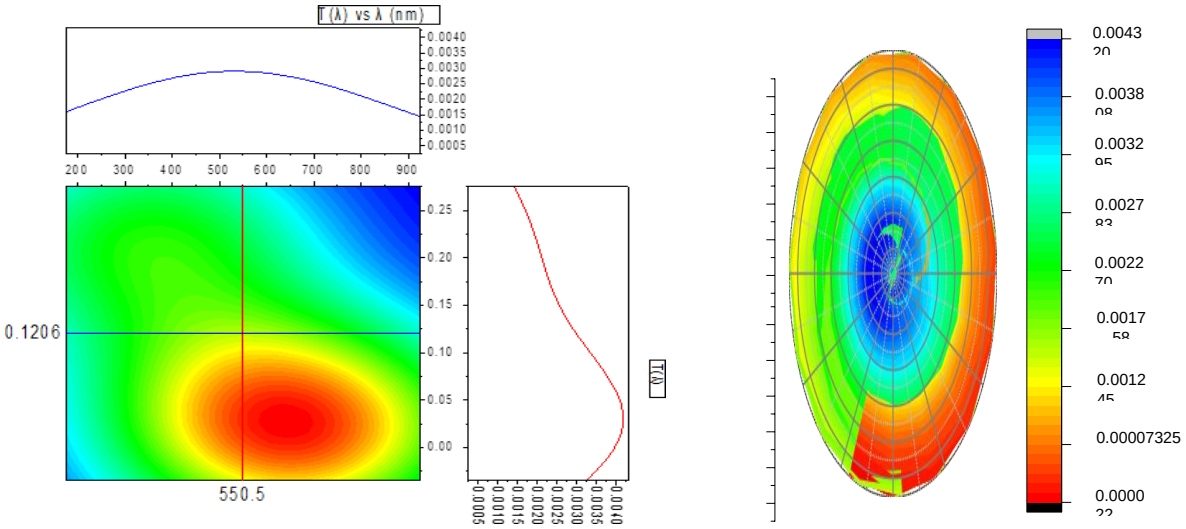

(a) (b)

Figure 4: (a) The maximum transmittance at 550.5 nm (b) Polar contour: θ(x) r(Y)

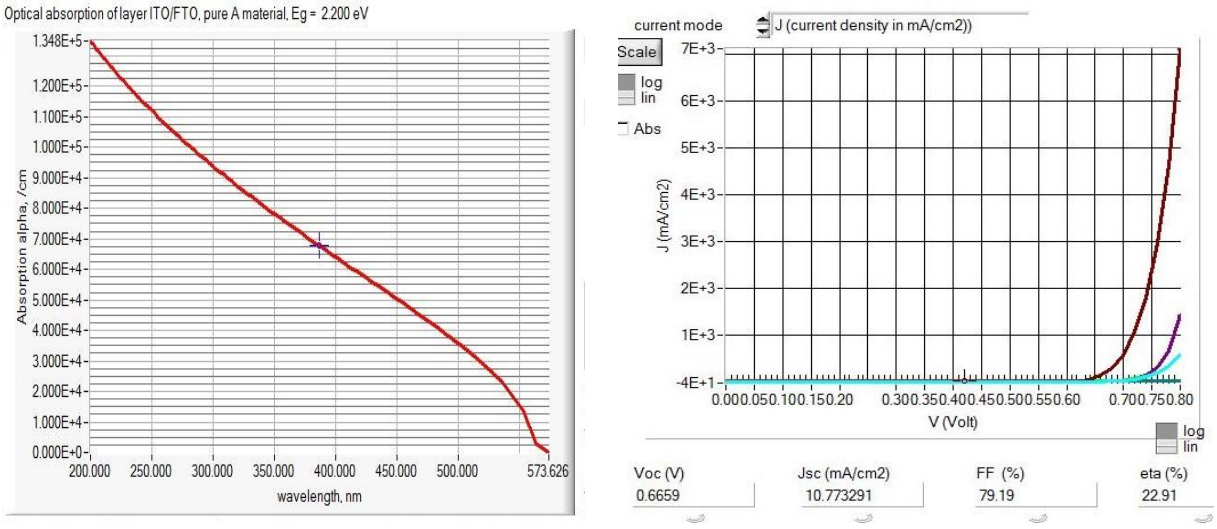

(a) (b)

Figure 5: (a) The optical absorption of the ITO/FTO layer (b) the J-V characteristics curve for second configuration

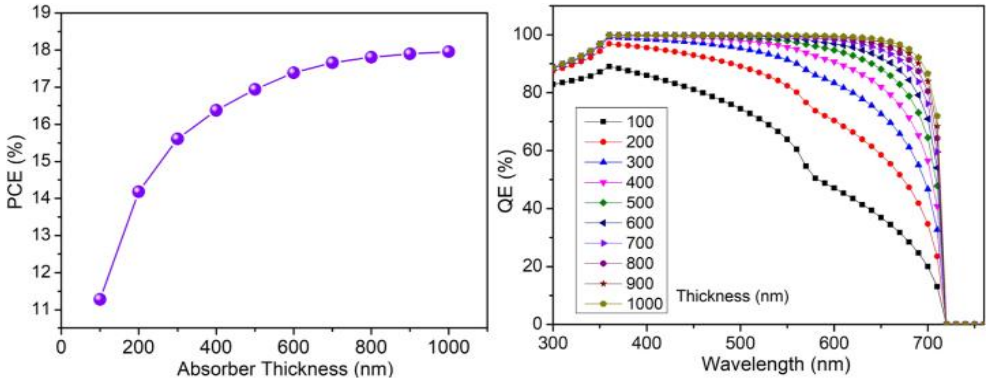

(a) (b)

Figure 6: The variation of PCE (a) and QE (b) with different absorber thickness

CONCLUSION

In this paper, graphene oxide was synthesized by modified Hummer's method and the optical properties were explored using UV-visible spectroscopy. The absorption coefficients at different wavelengths based on Beer-Lambert's law were determined and used in the design of lead-free methyl ammonium germanium halide solar cell using GO as carrier transporters. The numerical modelling of the device in SCAPS 1D program based on second order differential equation was carried out. For the first time, a 0.6227 V, 38.58 $mAcm^{-2}$, 83.07 %, 19.95 % were recorded as the open-circuit voltage, current density, fill factor and power conversion efficiency for FTO/GO/Perovskite/Cu_2O/Au and FTO/GO/TiO_2/Perovskite/Spiro-OMETAD/Au based design recorded 0.6659V, 10.77$mAcm^{-2}$, 79.19%, and 22.91% respectively. The investigation showed that the presence of graphene improved the optical transparency and enhanced carrier generation and interaction between other layers which optimizes the electrical conductivity and efficiency of the solar cells when compared to previous studies in literature. The results emphasized a viable approach to in the design of efficient and stable solar cells at a reduced cost and optical losses.

ACKNOWLEDGEMENT

We are thankful to Prof. Marc Burgelman and his group at the Department of Electronics and Information Systems (EIS), University of Gent, Belgium who developed SCAPS software used in this study and Mr. Muhammed Baba-Saje, Chemistry department, Nile University for his support during the synthesis of graphene using modified Hummer's method.

REFERENCES

Paulchamy B, Arthi G, Lignesh BD (2015) A Simple approach to stepwise synthesis of graphene oxide nanomaterial. J Nanomed Nanotechnology 6:253. https://doi.org/10.4172/2157-7439.1000253

Kumar, P., Divya, N., & Ratan, J. K. (2019). Synthesis and Characterization of Chemically Derived Graphene Oxide from Graphite. Sustainable Engineering, 85–94. https://doi.org/10.1007/978-981-13-6717-5-9

Chou J.C, Lin Y.J, Liao Y.H, (2016) Photovoltaic Performance Analysis of DSSC With ZnO Compact Layer and TiO_2/GO Composite Photoanode J. Electron Device soc., V4, No.6 https://doi.org/10.1109/JEDS.2016.2614940

Alam, S.N., Sharma, N., Kumar, L. (2017) Synthesis of GO by modified Hummer's method and its thermal reduction to obtain reduced graphene oxide (rGO). Graphene, 6, 1-18. https://doi.org/10.4236/graphene.2017.610

Chou, J.C., Chang, J.X., Ko, C.C., (2020). Improving DSSC performance using enhanced double layers based on magnetic beads and RGO. IEEE Transactions on Nan, 1-1. https://doi.org/10.1109/tnano.2020.2991413

Agresti, A., Pescetelli, S., Taheri, B. (2016). Graphene-Perovskite Solar Cells Exceed 18 % Efficiency: A Stability Study. Chem Sus Chem, 9(18), 2609-2619. https://doi.org/10.1002/cssc.201600942

Elseman, A.M., Shalan, A.E., Rashad, M.M. (2017). Experimental and simulation study for impact of different halides on the performance of planar PSCs. Mat. Sci. in Semiconductor Processing, 66, 176–185. https://doi.org/10.1016/j.mssp.2017.04.022

Gagandeep, Singh M., Kumar, R. (2020). Investigating the impact of layer properties on the performance of p-graphene/$CH_3NH3PbI3$/n-csi solar cell using numerical modeling. Super-lattices and Microstructures, 106468. https://doi.org/10.1016/j.spmi.2020.106468

Dadashbeik, M., Fathi, D., & Eskandari, M. (2020). Design and simulation of PSCs based on graphene and TiO_2/graphene nanocomposite as electron transport layer. Solar Energy, 207, 917-924. https://doi.org/10.1016/j.solener.2020.06.102

Daraie, A., & Fattah, A. (2020). Performance improvement of perovskite heterojunction solar cell using graphene. Optical Materials, 109, 110254. https://doi.org/10.1016/j.optmat.2020.110254

Kumar, N., Patel, S. R., & Gohel, J. V. (2018). Superior efficiency achievement for $FAPbI_3$-perovskite thin film solar cell by optimization with response surface methodology technique and partial replacement of Pb by Sn. Optik. https://doi.org/10.1016/j.ijleo.2018.09.066

Yang H.Y, Rho W.Y, Lee S.K. (2019) TiO_2 nanoparticles/nanotubes for efficient light harvesting in perovskite solar cells, Nanomaterials 9 https://doi.org/10.3390/nano9030326

Hummers, W.S., Offeman, R.E. (1958) Preparation of graphitic oxide, J.Am. Chem. Soc. 80, 1339-339 https://doi.org/10.1021/ja01539a017

Marcano, D.C, Dmitry V. K, Jacob M.B (2010) Improved Synthesis of GO, ACS Nano, V4, 8. https://doi.org/10.1021/nn1006368

Hazeghi F, Ghorashi SMB (2019) Mater. Res. Express. https://doi.org/10.1088/2053-1591/ab2f1b

Haidari, G. (2019). Comparative 1D opto-electrical stimulation of the perovskite solar cell. AIP Advances, 9(8), 085028. https://doi.org/10.1063/1.5110495

Lee, K. Lin, W.J., Chen, S.H., & Wu, M.C. (2019). Control of TiO_2 electron transport layer properties to enhance perovskite photovoltaics perf and st. Organic Electronics, 105406. https://doi.org/10.1016/j.orgel.2019.105406

Kazmi, S.A., Hameed S., Ahmed A.S., (2016) Electrical and optical properties of graphene-TiO_2 nanocomposite and its applications in DSSC, J.Alloys and Compounds. https://doi.org/10.1016/j.jallcom.2016.08.319

Baharin A., Sahari S.K., Kemat R. (2020). The Effects of TiO_2 and RGO Doping Ratio Variation to the Performance of DSSC Intl Jr of Nanoelectronics and Materials. V.13, No. 1, (159-168).

Eluyemi, M., Eleruja, M., Adedeji, A. (2016) Synthesis and Characterization of Graphene Oxide and Reduced Graphene Oxide Thin Films Deposited by Spray Pyrolysis Method. Graphene, 5, 143-154.

Kim, K., Yoo, J. S., Ahn, S. K., Eo, Y.-J., Cho, J.-S., Gwak, J., & Yun, J. H. (2017). Performance prediction of chalcopyrite-based dual-junction TSCs. Solar Energy, 155, 167–177. https://doi.org/10.1016/j.solener.2017.05.080

Jarwal, D. K., Mishra, A. K., Kumar, A. (2020). Fabrication and TCAD simulation of TiO_2 nano-rods electron transport layer based perovskite solar cells. Sup

and Micr, 106463. https://doi.org/10.1016/j.spmi.2020.106463

Kanoun, A.A., Kanoun, M.B., Merad, A.E. (2019). Toward development of high-performance PSCs based on $CH_3NH_3GeI_3$ using computational approach. Solar Energy, 182, 237-244. https://doi.org/10.1016/j.solener.2019.02.041

Hu, W., Yang, S., Yang, S. (2019). Surface Modification of TiO_2 for PSCs. Trends in Chem

Kumar, M., Raj, A., Kumar, A., & Anshul, A. (2020). An optimized lead-free formamidinium Sn-based perovskite solar cell design for high power conversion efficiency by SCAPS simulation. Optical Materials, 108, 110213. https://doi.org/10.1016/j.optmat.2020.110213

Paulson, P.D., Birkmire, R.W., & Shafarman, W.N. (2003). Optical characterization of $CuIn_{1-x}Ga_xSe_2$ alloy thin films by spectroscopic ellipsometry. J. App Phy, 94(2), 879-888. https://doi.org/10.1063/1.1581345

Tress, W., Domanski, K.,…Hagfeldt, A. (2019). Performance of perovskite solar cells under simulated temperature-illumination real-world operating conditions. Nature Energy https://doi.org/10.1038/s41560-019-0400-8

Wali, Q., Elumalai, N. K., Iqbal, Y., Uddin, A., & Jose, R. (2018). Tandem perovskite solar cells. Renewable and Sustainable Energy Reviews, 84, 89–110. https://doi.org/10.1016/j.rser.2018.01.005

Ladan H.M.A and Buba A.D.A (2021) Synthesis and Characterization of Graphene for Perovskite Solar Cells, Ph.D Thesis, Department of Physics, Faculty of Science, University of Abuja, Nigeria. www.uniabuja.edu.ng

Burgelman M., Nollet P., Degrave S., Modeling polycrystalline semiconductor solar cells, Thin Solid Films 361-362 (2000) 527-532.

Lakhdar, N., & Hima, A. (2019). Electron transport material effect on performance of perovskite solar cells based on $CH_3NH_3GeI_3$. Optical Materials, 109517. https://doi.org/10.1016/j.optmat.2019.10951

Mahajan, P., Datt, R., Chung Tsoi, W., (2020). Recent progress, fabrication challenges and stability issues of lead-free tin-based perovskite thin films in the field of photovoltaics. C. Chem Reviews, 213633.

Iqbal Z.M, Ali S.R., & Khan S., (2019) Progress in dye DSSC by incorporating natural photosensitizers, Solar Energy 181 (201) 490-509.

Geim, A.K. and Novoselov, K.S. (2007) The Rise of Graphene. Nature Materials, 6, 183-191.

Rao H., S. Ye, W. Sun, W. Yan, Y. Li, H. Peng, Z. Liu, Z. Bian, Y. Li, C. Huang, (2016) Nano Energy solar cells by an effective Cl doping method 27 51-57, https://doi.org/10.1016/j.nanoen.2016.06.044

Rai, S., Pandey, B. K., & Dwivedi, D. K. (2020). Modeling of highly efficient and low cost $CH_3NH_3Pb(I_{1-x}Cl_x)_3$ based PSCs by numerical simulation. Optical Mat., 100, 109631. https://doi.org/10.1016/j.optmat.2019.109631

Zhu Z., Y. Bai, X. Liu A.K.Y. Jen, (2016) Enhanced efficiency and stability of inverted PSCs using highly crystalline SnO_2 nanocrystals as the robust electron-transporting layer, Adv. Mater. 28 6478-6484.

Karthick, S., Velumani, S., & Bouclé, J. (2020). Experimental and SCAPS simulated formamidinium perovskite solar cells: A comparison of device performance. Solar Energy, 205, 349–357. https://doi.org/10.1016/j.solener.2020.05.041

Sutar D.S, G. Singh and V. D. Botcha, (2012) "Electronic structure of graphene oxide and reduced graphene oxide monolayers", Appl. Phys. Lett., 101, 103103

Wang, H., Wang, X., Zong, X. (2020). Organic-Inorganic Hybrid Perovskites: Game-Changing Candidates for Solar Fuel Production. Nano Energy, 104647. https://doi.org/10.1016/j.nanoen.2020.104647

Mandadapu U, S.V. Vedanayakam, K. Thyagarajan, Simulation and analysis of lead based perovskite solar cell using SCAPS-1D, Indian J. Sci. Technol. 10 (2017) 1-8, https://doi.org/10.17485/ijst/2017/v10i11/110721

Mudd, G. W., Svatek, S. A.…Patanè, A. (2015). High Broad-Band Photoresponsivity of Mech Formed InSe-Graphene van der Waals Heterostructures. Adv. Mat., 27(25),3760-3766. https://doi.org/10.1002/adma.201500889

Zhou, Y., Chen, J., Bakr, O. M., & Sun, H.-T. (2018). Metal-doped lead halide perovskites: synthesis, properties, and optoelectronic applications. Chemistry of Materials. https://doi.org/10.1021/acs.chemmater.8b02989

Zhang, P., Yang, F., Kamarudin.. Hayase, S. (2018). Performance enhancement of mesoporous TiO_2-based PSCs by SbI_3 interfacial modification layer. ACS App Mat. & Interfaces. https://doi.org/10.1021/acsami.8b10062